


Article

The Innovative Research on Sustainable Microgrid Artwork Design Based on Regression Analysis and Multi-Objective Optimization

Shuang Chang ^{1,*}, Dian Liu ¹ and Bahram Dehghan ² ¹ School of Design and Art, Xijing University, Xi'an 710123, China; 20150114@xijing.edu.cn² Department of Electrical Engineering, Sarvestan Branch, Islamic Azad University, Sarvestan, Iran; bahram.dehghan@iaau.ac.ir

* Correspondence: 20160062@xijing.edu.cn

Abstract: One of the most vital issues in electrical systems involves optimally operating microgrids (MGs) using demand-side management (DSM). A DSM program lowers utility operational costs in one sense but also needs policies that encourage financial incentives in the other. The present study formulates the optimum functioning of MGs using DSM in the form of a problem of optimization. DSM considers load shifting to be a viable option. There are operational limitations and executive limitations that affect the problem, and its objective function aims at minimizing the overall operational prices of the grid and the load-shifting prices. The major problem has been solved using an improved butterfly optimization scheme. Furthermore, the suggested technique was tested in various case studies that consider types of generation unit, load types, unit uncertainties, grid sharing, and energy costs. A comparison was made between the suggested scheme and various algorithms on the IEEE 33-bus network to demonstrate the proficiency of the suggested scheme, showing that it lowered prices by 57%.

Keywords: demand-side management; improved butterfly algorithm; optimal operation; microgrid; load shifting



Citation: Chang, S.; Liu, D.; Dehghan, B. The Innovative Research on Sustainable Microgrid Artwork Design Based on Regression Analysis and Multi-Objective Optimization. *Systems* **2023**, *11*, 354. <https://doi.org/10.3390/systems11070354>

Academic Editor: Morteza Dabbaghjamanesh

Received: 31 May 2023
Revised: 1 July 2023
Accepted: 4 July 2023
Published: 11 July 2023



Copyright: © 2023 by the authors. Licensee MDPI, Basel, Switzerland. This article is an open access article distributed under the terms and conditions of the Creative Commons Attribution (CC BY) license (<https://creativecommons.org/licenses/by/4.0/>).

1. Introduction

There are many challenges facing the current electric grid, such as conserving power, improving flexibility, reducing emissions from traditional energy production, reducing fossil fuel consumption, optimizing environmental and economic effects, etc. Different distributed energy resources (DERs) can be integrated with a smart microgrid (MG) to address such problems. MGs consist of various loads and energy storage systems, as well as renewable and small-scale dispatchable energy systems like microturbines (MTs), photovoltaic (PV), wind turbines (WTs), diesel engine generators (DEs), fuel cell (FCs), and so on [1,2]. An important part of the smart grid system is the MG's energy production manner. Most MGs operate in either islanded or grid-connected modes. MGs use renewable energy resources (RERs) as their main energy production resources, and these resources tend to be intermittent. An MG's uncertainty is typically caused by supply and demand, due to the unpredictable behavior of RERs and the MG's total load demand. This uncertainty makes balancing the energy between the overall production and load demand at the MG an important challenge. It is feasible to solve the problem of their unpredictable nature by implementing DSM strategies using different RERs. DSM schemes will be essential for today's smart grids in order to manage the excess power requirements of users while also minimizing imbalances between energy production and load consumption. In order to implement DSM successfully, modern metering systems and communication and information technologies must be utilized [3]. Various price policies have been discussed by researchers regarding DSM load shifting, including real-time costing, acute peak costing, slope block

rate, and time of use (ToU). Energy management will be essential for improving reliability, quality of power, sustainability, and ensuring reliable, economic, and environmentally friendly functioning in the MG [4,5].

The optimum MG efficiency and energy management issues have been extensively studied by researchers. Refs. [6,7] examined an online multi-objective optimization method using a revised game theory framework in order to improve both the environmental and economic goals of MG operations. Ref. [4] integrated the stimulus-driven demand response program with the MG energy-management problem in order to optimize dispatch methods. Ref. [1] applied four types of optimization methods in order to optimize MG: direct quest, particle swarm optimization, lambda logic, and iteration. Ref. [8] examined a combination of economic dispatch and a DSM scheme for an MG system with the aim of minimizing the entire price for household users. The MG optimum operational problem must account for uncertainty in supply and demand in order to obtain optimal planning. Ref. [9] applied Monte Carlo simulation for handling the uncertainty associated with unpredictable power resources and load. Ref. [10] used a linear two-step stochastic scheme in an uncertain environment in order to optimize MG operation. MG operating optimization problems have been discussed in several studies. The majority of investigations fail to adequately analyze the effects of domestic DSM strategies on MG operations and users' satisfaction level objectives are not adequately addressed in their DSM methods.

Ref. [11] examined a probability-based day-ahead EMS approach for scheduling the MG network's dispatchable and non-dispatchable power resources. That study used a pumped-storage unit and a stimulus-driven DRP for maintaining the production and load balance. Ref. [12] examined the effects of stimulus-based DR schemes on the intra-day and day-ahead markets. Instead of selecting values for static elastic coefficients used in that study, it may be possible to model users' reactions to cost variations more realistically. Ref. [13] examined the effect of DRPs on network resilience using several MGs. Stochastic EMS in that study took into account not only the operational planning but also indicators of the reliability of local loads during an emergency. Ref. [14] combined optimum planning of tidal energy resources into a probabilistic EMS architecture using DRP, resulting in a reduction of 13.14 percent in overall operational prices.

The purpose of the present study is to formulate the problem of optimum operation of MGs and demand-side management (DSM) through the development of common strategies for electric grid operations and consideration of the required limitations. The objective function (OF) aims at minimizing operation prices and DSM prices, and optimization limitations consist of generator limitations and restrictions on energy balance. Additionally, the hours of load shifting are taken into account as variables, and an improved butterfly optimization algorithm (IBOA) is applied for solving the optimization problem. This paper is divided as follows: Section 1 introduces the DSM, Section 2 defines the OF and formulation scheme, Section 3 presents the problem-solving approach, Section 4 presents the simulation outcomes, and Section 5 presents the conclusion.

2. Problem Formulations

An optimization problem is proposed for optimum unit production scheduling. An MG's optimum operating strategy takes into account both the minimum price and operational limitations as well as DSM limitations. The OFs in the problem consider the overall production prices and the prices of using DSM. As a result, Equation (1) is used to define the OF of the problem of optimum operation of MGs taking DSM into account [15]:

$$\min F = \omega_1 \times OC + \omega_2 \times DC \quad (1)$$

in which F shows the overall operation prices for the MG, OC represents the overall operational costs (OC) of the energy production units, and DC represents the overall price to implement the demand-side programs. ω_1 and ω_2 show the weight ratios of the operation prices of the system and the price to implement DSM programs, respectively.

Subscriber dissatisfaction is caused by the use-time variation scheme. Therefore, the present study models the price to implement the load-shifting program as the discomfort function as a 3-degree function based on Equation (2):

$$DC = \sum_{l=1}^m [A_l st_l^3 + B_l st_l^2 + C_l st_l] \quad (2)$$

in which l represents the number of loads capable of shifting, A , B and C represent the price of shifting for the load, st_l shows the times of loads l transferring, and m represents the overall number of shiftable loads. The operational cost of a production unit includes the cost of production, the cost of startup, and the cost of maintenance. Moreover, since power can be bought or sold to the utility in the MG, the price of purchasing or selling energy to the grid appears in the operational cost function. An OC operational cost function is shown in Equation (3) for the optimization problem [16]:

$$CF = \left(\sum_{t=1}^T \sum_{i=1}^I C(i, t) + MC(i, t) + SC(i, t) \right) + \sum_{t=1}^T [C(t) - R(t)] \quad (3)$$

in which $C(i, t)$ indicates the price to generate energy of agent i for time t of operating, $MC(i, t)$ indicates the price of maintenance, and $SC(i, t)$ indicates the price of beginning agent i for time t . In addition, $C(t)$ represents the price to purchase energy for time t from the network, and during that time, $R(t)$ represents power sales revenue. I shows the number of energy production agents and T represents the study time ($T = 24$) in hours. I includes many production units like PV, WT, MT, FC, and battery, with diverse cost functions. WT output power can be calculated based on wind speed using Equation (4) as follows:

$$P_{WT} = \begin{cases} 0 & 0 < V < V_{ci} \\ (a \cdot V^2 + b \cdot V + c) * P_r & V_{ci} < V < V_r \\ P_r & V_r < V < V_{co} \\ 0 & V_{co} < V < \infty \end{cases} \quad (4)$$

In this equation, the parameter P_r represents the rated power of WT, V_{ci} shows minimum permitted wind speed, V_{co} represents maximum permitted wind speed, V_r shows the nominal velocity, and V represents the real wind velocity. a , b and c can be found from a current device's catalog. Solar cells generate energy based on light intensity and ambient temperature and the relevant values can be determined based on Equation (5):

$$P_{PV} = P_{STC} * \frac{G_{INC}}{G_{STC}} * (1 + k(T_C - T_r)) \quad (5)$$

in which P_{PV} represents solar cell output power in terms of area irradiance severity, P_{STC} shows maximal cell production energy in standard trail statuses, G_{INC} shows area light severity, G_{STC} represents irradiance severity in standard trail statuses, k shows output power temperature ratio, T_r and T_C show reference and cell temperatures. Wind and solar energy are used rather than fuel as the RERs of WTs and PVs. Due to this, there are no fuel expenses associated with such units. Aside from the substantial construction costs, maintenance costs must also be taken into account when assessing the economics of MGs. Therefore, Equation (6) is used to calculate the overall price of WTs and PV units:

$$C_{RES} = \sum_{t=1}^{24} P_{WT,t} * \left(AC * I_{WT}^{Inv} * I_{WT}^M \right) + \sum_{t=1}^{24} P_{PV,t} * \left(AC * I_{PV}^{Inv} * I_{PV}^M \right) \quad (6)$$

in which C_{RES} shows the price of renewable units, AC shows the yearly price factor, I^{Inv} is coefficient of investiture price to produce the energy of the agent, I^M shows agent repair price.

A governor controls the DE's output power. As the second-class function of producing power, DE fuel usage (L/h) can be given by Equation (7):

$$C_{DE} = \alpha \cdot (P_{DE})^2 + \beta \cdot P_{DE} + \gamma \quad (7)$$

in which, C_{DE} shows DE fuel usage price L/h , P_{DE} shows the output power of DE, α , β , and γ would be constant. Based on Equation (8), performance of FC equals the output power to the input fuel when they are computed in a similar unit:

$$C_{FC} = C_{gasFC} * \frac{P_{FC}}{\mu_{FC}} \quad (8)$$

in which C_{FC} shows the price of fuel utilized via a FC (USD/h), C_{gasFC} represents the price of natural gas for feeding the FC (USD/kWh), P_{FC} shows the FC output power, μ_{FC} shows the FC performance. Based on Equation (9), an MT has the same economic scheme as an FC, but its performance improves as power rises:

$$C_{MT} = C_{gasMT} * \frac{P_{MT}}{\mu_{MT}} \quad (9)$$

Equations (10) and (11) are used to express the price of power bought $C(t)$ and sold $R(t)$ (Equation (3)):

$$C(t) = T_{pp} \times P_{pp} \quad (10)$$

$$R(t) = T_{sp} \times P_{sp} \quad (11)$$

T_{pp} represents the tariff to purchase power from the network, P_{pp} shows the energy bought from the network, T_{sp} shows the tariff to sell power to the network, and P_{sp} shows the electricity sold to the network. The price to repair and maintain units depends directly on their energy production. Thus, the price of repairing and maintaining unit i for time t can be determined by Equation (12):

$$MC(i, t) = P(i, t) \times K(i) \quad (12)$$

in which $K(i)$ shows the cost of repairing and maintaining agent i per kW of electrical power and $P(i, t)$ represents the output power of agent i per hour t . Only fossil fuel production units are included in the start-up price. Based on the fact that the start-up price of agent i depends on the cycle during which the unit is operational, Equation (13) calculates the start-up price of agent i for time t :

$$SC(i, t) = S_{cost}(i) \times (U(i, t) - U(i, t - 1)) \quad (13)$$

in which $S_{cost}(i)$ shows the start-up price of agent i and $U(i, t)$ shows a binary parameter indicating the mode of agent i including off/on for time t . Coequality limitations in the problem would include the power equilibrium limitation, based on Equations (14) and (15):

$$P_k^G - P_k^L = \sum_{i=1}^N V_k V_i [G_{ki} \cos(\theta_k - \theta_i) + B_{ki} \sin(\theta_k - \theta_i)] \quad (14)$$

$$Q_k^G - Q_k^L = \sum_{i=1}^N V_k V_i [G_{ki} \sin(\theta_k - \theta_i) + B_{ki} \cos(\theta_k - \theta_i)] \quad (15)$$

Inequality limitations are agent output power limitations, control parameter limitations, line power limitations, and voltage limitations, and can be determined by Equations (16)–(19):

$$P^{min} \leq P \leq P^{max} \quad (16)$$

$$U^{\min} \leq U \leq U^{\max} \quad (17)$$

$$|P_{ij}| \leq P_{ij}^{\max} \quad (18)$$

$$V_j^{\min} \leq V_j \leq V_j^{\max} \quad (19)$$

Equation (20) considers the shifting time of all loads as a further limitation in the demand response program:

$$st_l \leq T_l \quad l = 1, \dots, m \quad (20)$$

in which T_l is the allowed time for shifting the load l th. This optimization problem can be transformed into the optimum power flow (OPF) problem through knowing the load shift time. As a result of resolving the OPF issue, it will be possible to determine the power produced via all units, as well as the power sent and received by the global network. The present study applies the IBOA for solving the optimization issue.

3. Improved Butterfly Optimization Algorithm

Smell, taste, and hearing are several of the senses that butterflies use to find food or mating partners, lay eggs, and escape hunters. Research indicates that butterflies have a strong sense of smell, particularly when searching for food from afar [17].

Chemoreceptors are nerve cells that are responsible for butterflies' ability to search for food. The butterfly's chemoreceptors are utilized to smell and are distributed throughout its body. The butterfly also uses this sense to find the right mate for itself [18]. Butterflies are capable of sensing, locating, and even separating various fragrances [19]. Aroa and Singh developed the butterfly optimization algorithm (BOA) [20]. The BOA's population consists of butterflies acting as search agents. The BOA's OF price changes according to the position of the butterflies. Using the BOA, all butterflies share their experiences with their neighbors according to fragrances distributed across distances.

When the butterfly senses the scent of the other butterfly, it follows it by using the stage as a universal quest spot. Butterflies are subjected to another movement as part of their local search optimization. Generated randomness is used for this part. By balancing the smell senses and fragrance, the BOA is applied.

3.1. Fragrance

There are three sections to fragrance: power exponent, sensory modality, and stimulus intensity. I indicates the physical incentive size which has been associated via the fitness solution, i.e., when the butterfly emits lots of fragrance, the surrounding butterflies are able to sense and are attracted to it.

Two important factors contribute to butterflies' substance: changes in fragrance formulation (f) and incentive intension (I). The below equation describes the fragrance scheme:

$$f = cI^\beta \quad (21)$$

in which f shows the observed extent of the fragrance, I shows the incentive intension, c is the sensory modality, and β shows the power exponent based on defining the changing level of attraction. β and c fall within $[0, 1]$.

3.2. Butterfly Movement

The BOA consists of three stages: the initialization, the questing, and the finalizing phases. The BOA evaluates OF values for all butterflies following the initialization of the primary butterfly swarm. The step also involves setting the parameters of the algorithm. The algorithm begins to optimize once the parameters have been assigned. A random position has been generated in the quest area for the butterflies. Artificial butterflies travel

to the updated places in the quest area once the iteration begins, and their prices are calculated. The next equation is used to produce the fragrance by butterflies in their places:

$$x_i^{t+1} = x_i^t + (r^2 \times g^* - x_i^t) \times f_i \quad (22)$$

in which g^* shows the optimal solution for the iteration t , x_i^t shows the solution vector x_i for i^{th} butterfly, the fragrance of the i^{th} butterfly is shown via f_i and r shows a randomly selected firm within zero and one. The local quest in the algorithm would be:

$$x_i^{t+1} = x_i^t + (r^2 \times x_j^t - x_k^t) \times f_i \quad (23)$$

in which x_j^t and x_k^t show the j^{th} and k^{th} members of the butterfly swarm in the quest area. Food search and partner mating in butterflies are BOA variables that take place both on a global and local scale.

The BOA is effective when it comes to exploring optimum values, but it fails when it comes to converging. This paper proposes a novel technique for modifying the BOA's key variables to increase convergence speed.

According to chaos theory, a vector of the BOA's key variables $V = [a, c, r]$ is used as the solution.

In chaos theory, unexpected and random patterns are studied. A chaotic system is a very sensitive dynamic system influenced by even the smallest change. The technique improves the point distribution in the search space by generating points with fewer complexities and greater distributions. The BOA's convergence speed is improved by the feature. Here is a general formulation of chaos theory:

$$V_{t+1}^j = f(V_i^j), j = 1, 2, \dots, l \quad (24)$$

in which l shows the map extent and $f(V_i^j)$ indicates the chaotic scheme producer function. A sinusoidal chaotic map was used as the main parameter in the following way:

$$\begin{aligned} a &= \alpha_1 p_i^2 \sin(\pi p_i) \\ c &= \alpha_2 p_i^2 \sin(\pi p_i) \\ r &= \alpha_3 p_i^2 \sin(\pi p_i) \end{aligned} \quad (25)$$

$$p_0 \in [0, 1], \alpha_1, \alpha_2, \alpha_3 \in (0.4], i = 1, 2, 3$$

Figure 1 depicts the flowchart for the IBOA.

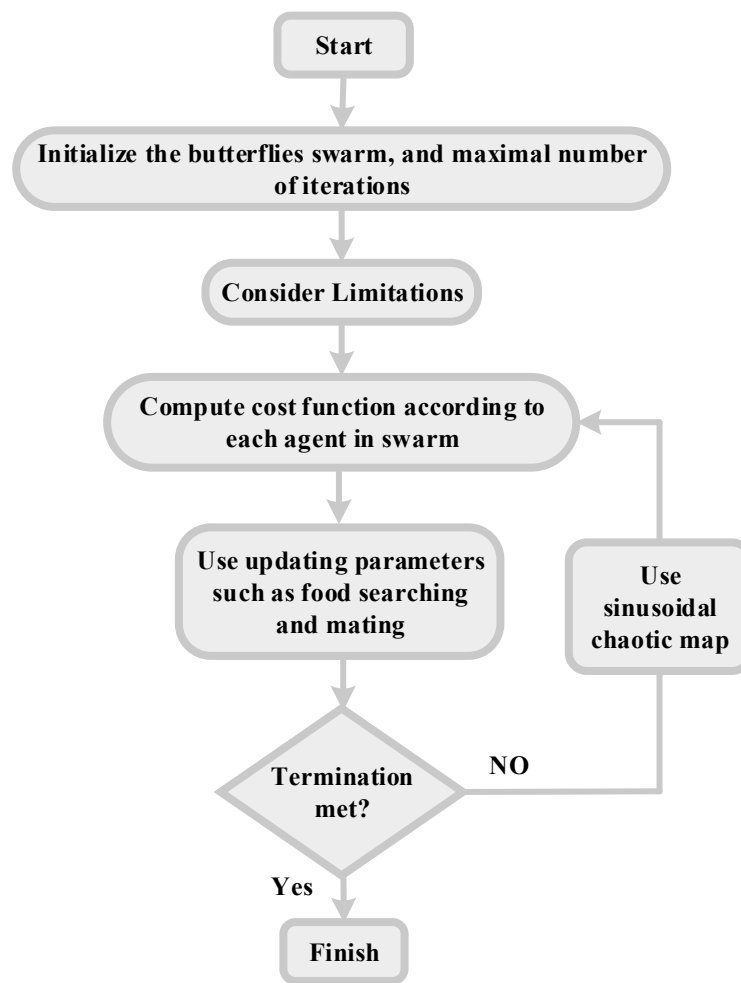


Figure 1. Block diagram for the suggested IBOA.

4. Simulation Outcomes

The following part presents the outcomes of evaluating the suggested approach in various scenarios. Figure 2 shows a sample of the MG presented in the study. From the PCC point, it has been linked to the main grid. There is a DE, a PV panel, and a number of loads on the grid.

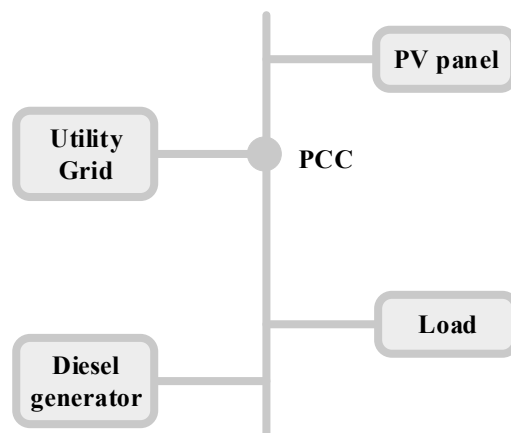


Figure 2. The first suggested MG.

The data concerning DEs are shown in Table 1. The PV power production curve over a day is shown in Figure 3. As can be seen in the figure, the PV generates power only at

hours with adequate access to solar irradiance. Therefore, there is a shut-down time for the PV overnight which will later be compensated by the dispatchable units. The power purchasing and sale costs are shown in Figure 4, and critical loads and shiftable loads are shown in Figure 5. The daily costs of purchasing and selling electric power from the grid in USD/h are shown in Figure 4. Power sold to the network equals 40 \$/h [9], and power bought from the network equals 60 \$/h [9] when costs stay constant. The coefficients to implement the DSM program are shown in Table 2.

Table 1. DE Data [21].

Production agent	Diesel generator
Minimum power	100 kW
Maximum power	4000 kW
Cost function	$F(p) = 0.02268p^2 + 15.06p + 817.47$

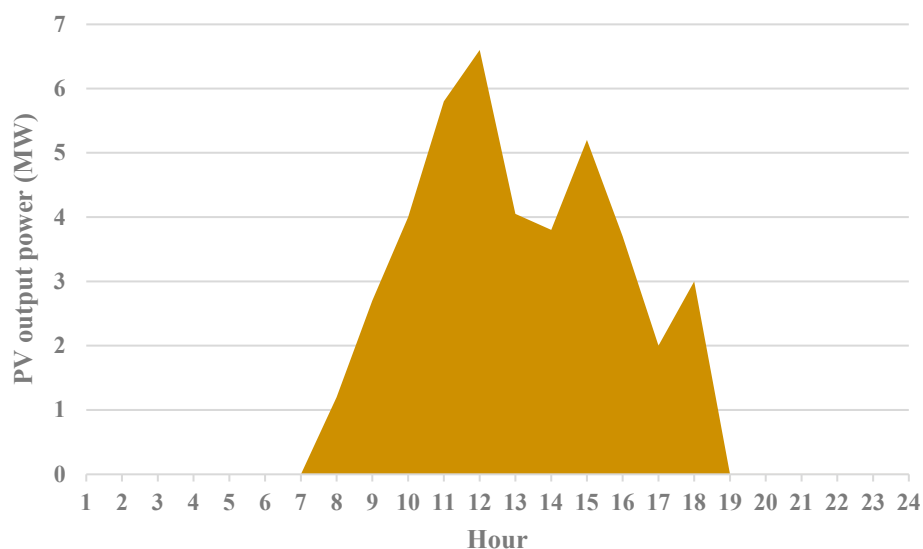


Figure 3. PV power production curve.

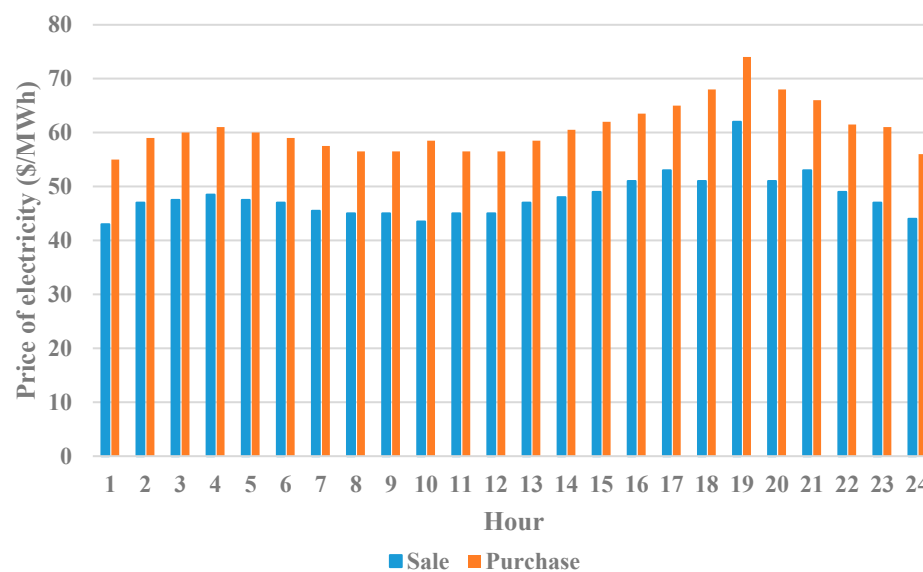


Figure 4. Purchasing and sale costs of power.

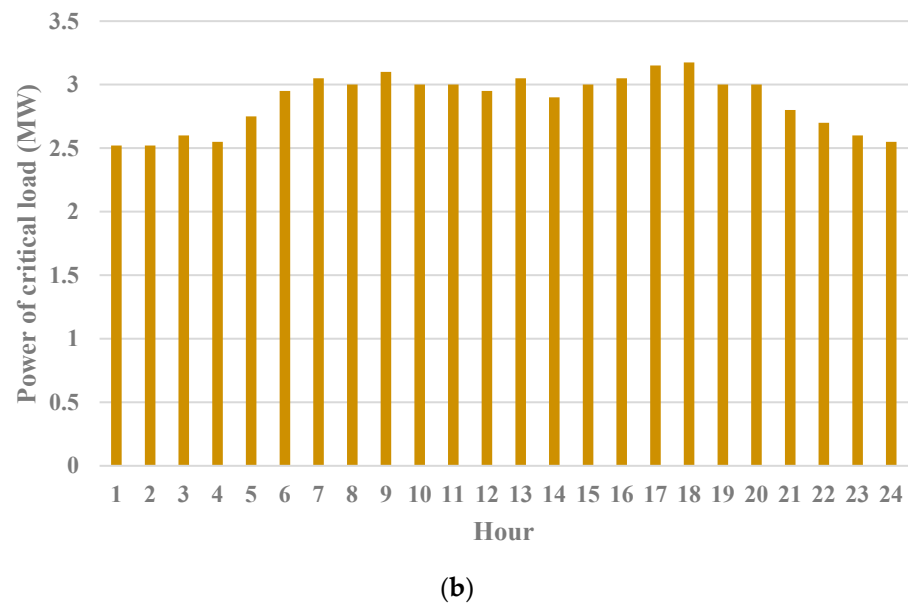
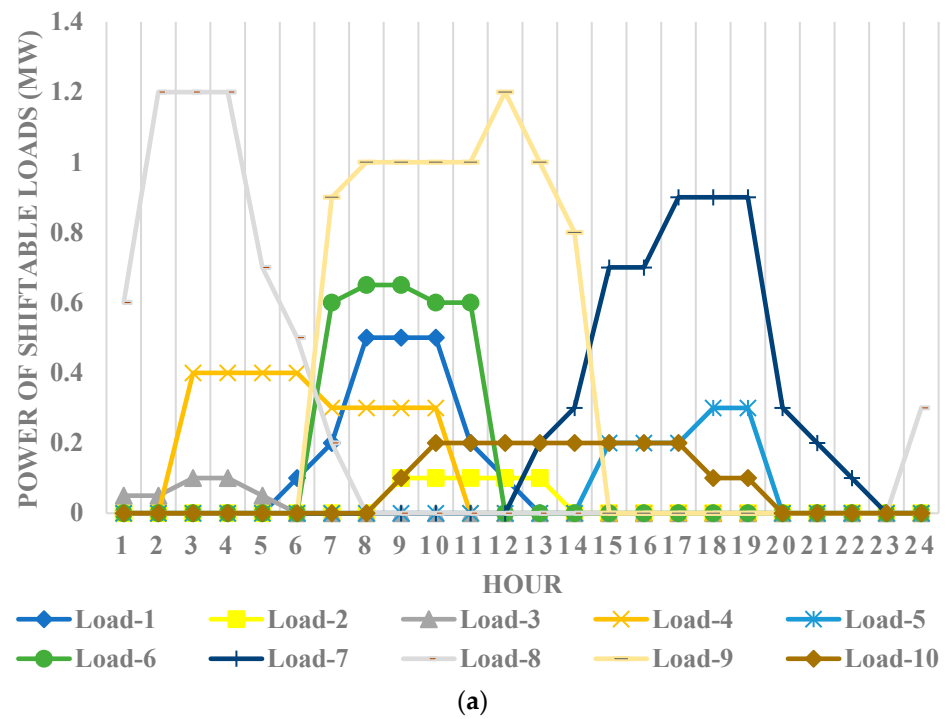


Figure 5. Loads data: (a) shiftable load, (b) non-shiftable load.

Table 2. Factors of DSM cost function [21].

Load	1	2	3	4	5	6	7	8	9	10
A	0	0	0	0.032	0	0	0.02	0	0	0
B	0.23	0.53	0.61	0.96	0.52	0.11	0.33	0.25	0.16	0.48
C	1	2	1	5	3	4	5	3	2	3

4.1. Implementing the Suggested IBOA Scheme

The following part illustrates the implementation of the suggested algorithm on a network in Figure 2. Here, ω_1 and ω_2 are weighting coefficients equaling 1, and the

purchasing and sale costs of energy are assumed to be variables (Figure 4). The population was equal to 500, and 200 iterations were performed.

Table 3 and Figure 6 give the outcomes of using the suggested algorithm. Every load’s shifting amount, the OC, and the DSM cost (DC) are shown in Table 3. In Figure 6, the output power of MG units is shown along with the energy supplied by the network.

Table 3. Load’s shifting amount and costs.

Time of Loads Shifting Regarding Hours				Costs		Coefficients	
ST_1	3	ST_6	1	DC (\$)	53,820	W_1	1
ST_2	0	ST_7	0	OC (\$)	3,081,652.3	W_2	1
ST_3	1	ST_8	8	F	3,135,472.3		
ST_4	0	ST_9	2				
ST_5	0	ST_{10}	0				

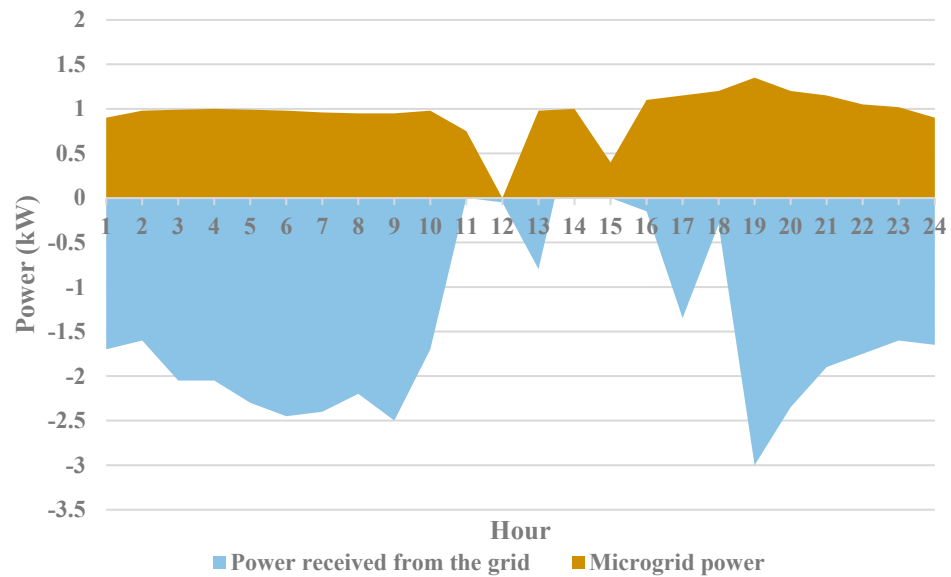


Figure 6. MG power production and energy supplied by the network.

We evaluated and analyzed the effects of weighting coefficients, PV panels, and energy prices on operation prices and the price of DSM programs.

4.2. Weighting Coefficients’ Impact

The operation price and the price to implement the DSM program are included in the OF of the optimization problem. These weighting coefficients were adjusted to estimate how every section impacts the overall price. This was accomplished by changing the weighting coefficients in accordance with Table 4; the outcomes are presented.

Table 4 assumes that the operation price has a weighting ratio of 1, whereas the price of DSMs has a weighting coefficient of 2. Load shifting becomes non-cost when ω_2 equals 0. There is no doubt that in this state, the minimum operation price and most load shifting were achieved. When the weight coefficients equal 1, operation prices increase, and load shifting decreases in comparison with the prior case.

Table 4. Weighting Coefficients' Impact on the OF.

Coefficients	W_1	1	1	1	Sans DSM
	W_2	0	1	2	
Time of load shifting, hours	ST_1	6	3	0	-
	ST_2	0	0	1	-
	ST_3	5	0	0	-
	ST_4	6	0	0	-
	ST_5	17	0	1	-
	ST_6	4	1	0	-
	ST_7	17	0	0	-
	ST_8	9	8	1	-
	ST_9	2	2	0	-
	ST_{10}	23	0	0	-
Prices	F	3,016,445	3,135,472.3	3,193,278.2	3,144,023.3
	OC (\$)	3,016,445	3,081,652.3	3,174,678.2	3,144,023.3
	DC (\$)	0	53,820	18,600	-

4.3. PV Panels' Effects

The results in Table 5 illustrate the effects of PV panels on the optimum function of the MG with and without PV panels. Based on the table, load transfer decreases as well as the price of DSM schemes without PV panels compared with the system with PV panels; however, operation costs increase considerably without PV panels. Due to the removal of PV panels, the DE supplies the entire power for the system.

Table 5. PV Panels' Effects on the OF.

	PV	Sans PV	Using PV
Time of load shifting, hours	ST_1	1	3
	ST_2	1	0
	ST_3	1	0
	ST_4	0	0
	ST_5	0	0
	ST_6	0	1
	ST_7	1	0
	ST_8	4	8
	ST_9	0	2
	ST_{10}	0	0
Prices	F	5,582,978.2	3,135,472.3
	OC (\$)	5,556,267.2	3,081,652.3
	DC (\$)	26,720	53,820

4.4. Energy Costs' Effects

The following part solves the optimization problem by considering fixed costs for the purchase and sale of power at various hours of the day and night, as illustrated in Figure 4. Table 6 shows the outcomes of implementing the two scenarios. Price stabilization enhances load shifting, and DSM program implementation costs increase but operating costs decrease.

4.5. Comparing IBOA Efficiency

The following part evaluates and validates the effectiveness of the suggested IBOA by implementing it on MGs using various kinds of production units and comparing the outcomes to a number of meta-heuristic algorithms. The second low-voltage MG investigated is shown in Figure 7. PV, WT, MT, and FC units were employed for energy production in this MG, while batteries were employed for power storage and energy production resources for other MGs. Table 7 shows all production units' ranges of power.

Ref. [22] provides network data, such as load demand, energy costs, and so on. Table 7 shows that negative power for batteries indicates the batteries will store power and that negative value for the grid indicates the MG will sell power to the main grid.

Table 6. Energy Costs’ Effects on the OF.

Cost		Constant	Changeable
Time of load shifting, hours	ST ₁	3	3
	ST ₂	1	0
	ST ₃	1	0
	ST ₄	0	0
	ST ₅	0	0
	ST ₆	1	1
	ST ₇	0	0
	ST ₈	8	8
	ST ₉	3	2
	ST ₁₀	1	0
Prices	F	3,091,198.29	3,135,472.3354
	OC (\$)	3,026,958.2900	3,081,652.3354
	DC (\$)	64,240	53,820

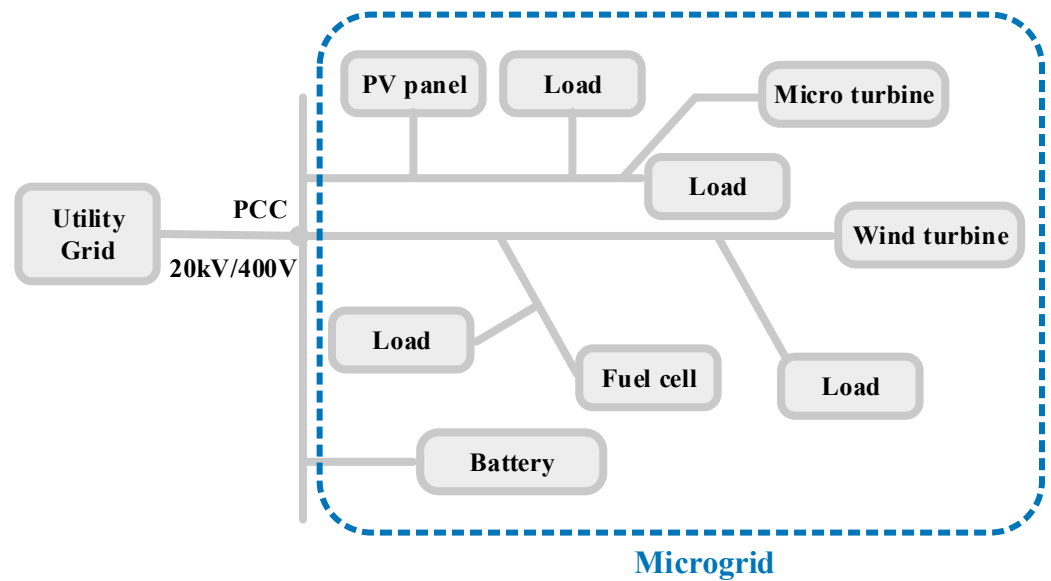


Figure 7. The second MG investigated.

Table 7. Range of power variations of production units.

Units	WT	FC	Grid	PV	MT	BAT
P_{max} (kW)	15	30	30	25	30	30
P_{min} (kW)	0	3	−30	0.33	6	−30

Figures 8 and 9 show the output of the suggested scheme as the production power of MG agents, price decrease, and DSM outcomes. The MG and main grid production power are shown in Figure 8, and the network load profile variations due to DSM are shown in Figure 9.

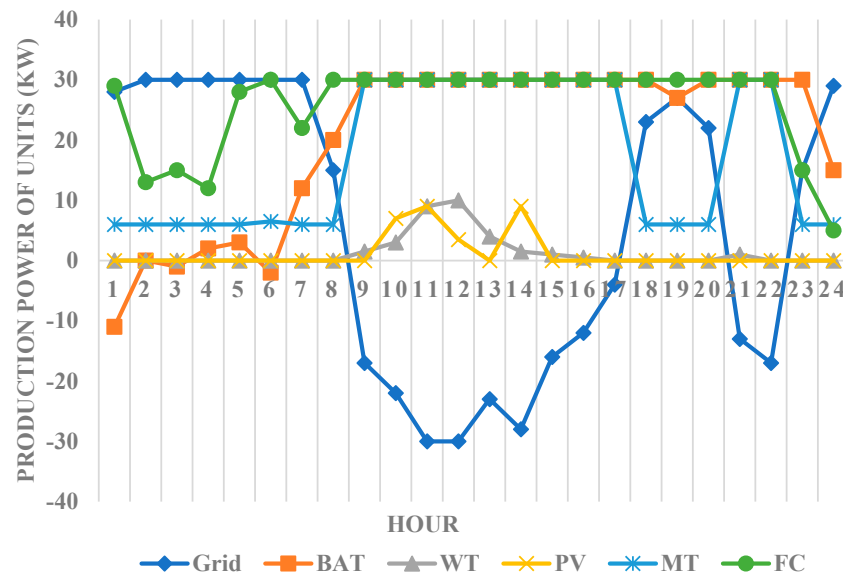
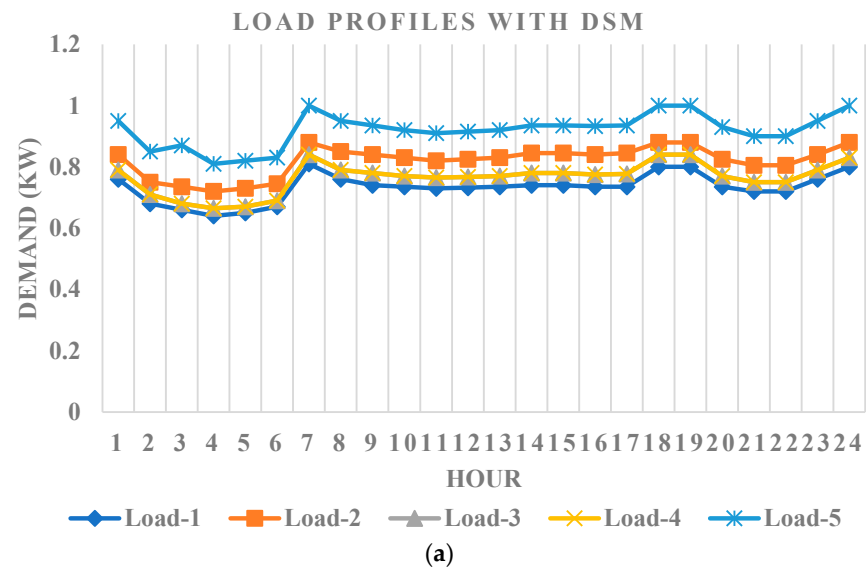
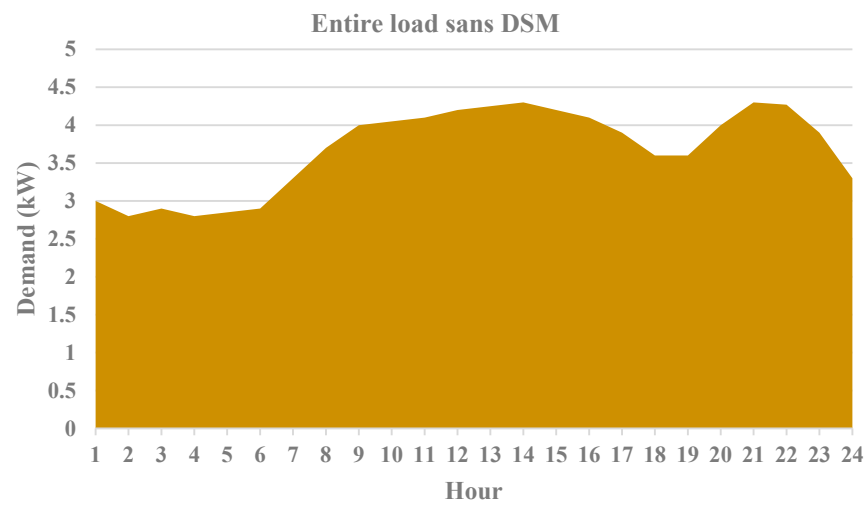


Figure 8. Production power of MG and main grid.



(a)



(b)

Figure 9. Network load variations in 24 h: (a) loads profile with DSM. (b) entire load sans DSM.

4.6. Implementing the Suggested Scheme on the Standard 33-Bus IEEE System

The following part demonstrates the effectiveness of the proposed scheme by applying the standard IEEE 33-bus network for a variety of units. There are four DG units, two combined heat and power (CHP) agents, one WT agent, and one PV agent in the MG, and it has been linked to the utility by buses [1,20]. Figure 10 depicts a revised 33-bus IEEE MG, capable of buying or selling energy. Table 8 presents the details of the DG units linked to buses 2, 7, 8, and 25 MGs. SD_c shows the price of starting and SU_c represents the price of stopping, R_{up} shows the rising slope rate and R_{dn} represents the dropping slope rate of unit generation, P_{max} shows the minimal generation capacity and P_{min} shows the maximal generation capacity of the units. CHPs can be found in buses 8 and 16, and since CHPs have restricted capacity, Table 9 indicates the minimal and maximal amount of energy and heat produced by the two units, as well as the constant coefficients of a cost function. A day’s expected use of heat load is shown in Figure 11. It is shown that the peak electric load matches the peak heat load (H_{max}).

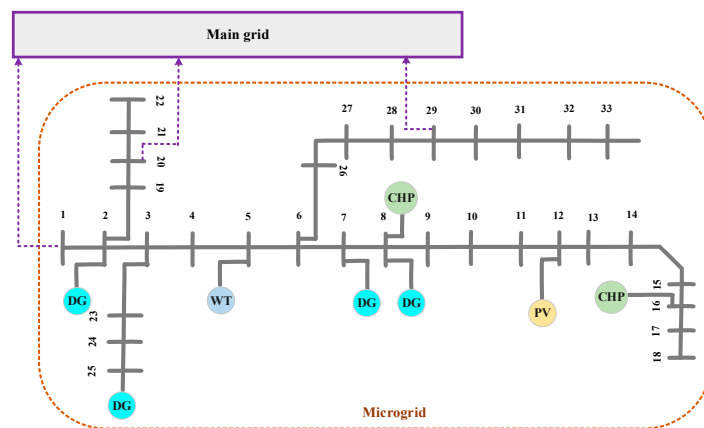


Figure 10. The third MG investigated (numbers show the bus number and lines are the feeders).

Table 8. Features of DG units.

Bus	25	8	7	2
R_{dn} (kW/H)	700	250	250	100
R_{up} (kW/H)	700	250	250	200
C_{DG} (\$/kWH)	50	35	45	27
SD_c (\$)	0	25	25	25
SU_c (\$)	0	50	20	20
P_{max} (kW)	400	500	550	400
P_{min} (kW)	50	20	40	50

Table 9. Features of CHP units.

Bus	16	8
A	0.0345	0.0435
B	14.5	36
C	26.5	12.5
D	0.03	0.027
E	4.2	0.6
F	0.31	0.011
H_{max} (kWth)	1356	1800
P_{max} (kW)	1258	2470
P_{min} (kW)	400	810

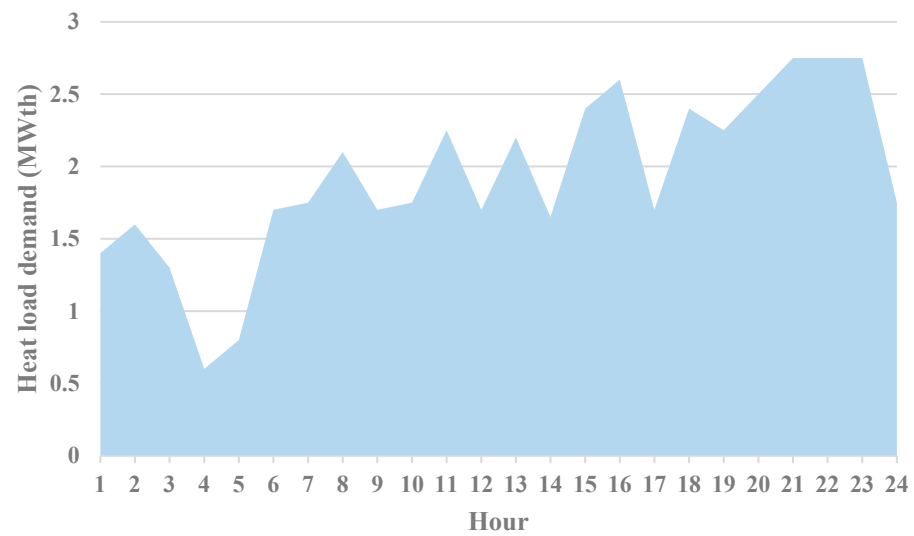


Figure 11. Estimated heat load demand over 24 h.

The following part compares the efficiency of the suggested scheme to other optimization techniques, using the third MG in four cases. The four cases are listed below:

- Case 1: With no consideration for DSM and in the absence of CHP agents in the MG.
- Case 2: With no consideration for DSM and using CHP units in the MG.
- Case 3: Through the consideration of DSM and in the absence of CHP agents in the MG.
- Case 4: Through the consideration of DSM and using CHP units in the MG.

Figure 12 shows the number of units involved and the energy received from the main grid in Case 1. Figure 12 shows that the MG usually purchases the most power from the utility via bus 1 during maximum demand. Moreover, having both WT and PV agents during 24 h would be a desirable condition for generation. As a result of the PV unit’s excellent performance daily from 8 AM to 5 PM, it produced enough electricity for 12 buses. In this case, the highest profit for MG would be USD 2185.7133.

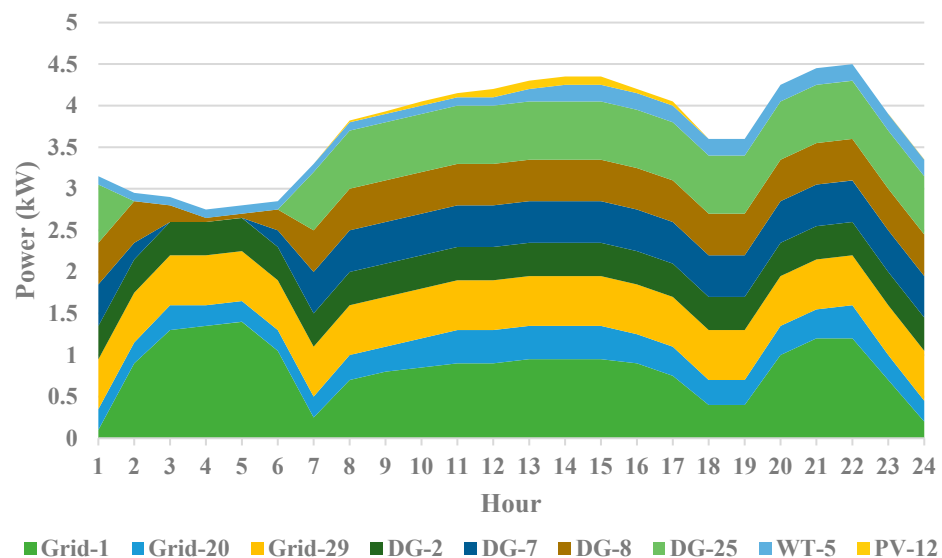


Figure 12. Unit involvement ratio in providing electric load for Case 1.

The agent involvement rate for Case 2 is shown in Figure 13. Because buses 8 and 16 have highly efficient CHPs, MG usually sells active power to the utility with a revenue of \$2682 and the maximum benefit equals \$5607.

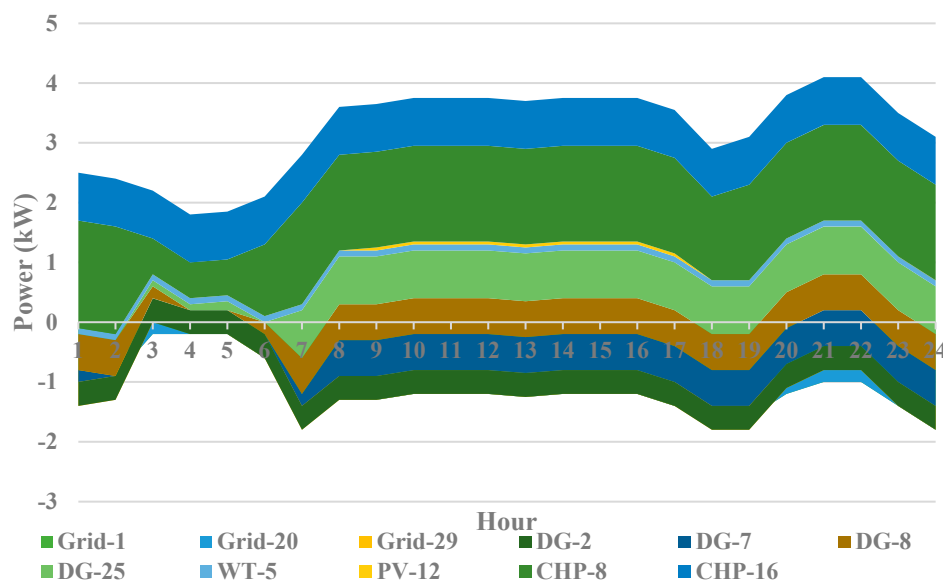


Figure 13. Unit involvement ratio in providing electrical loads for Case 2.

The involvement ratio of agents in Case 3 is shown in Figure 14. As a result of implementing DSM, the MG revenue grew by USD 2194.4, resulting in a profit of \$8.7 over Case 1.

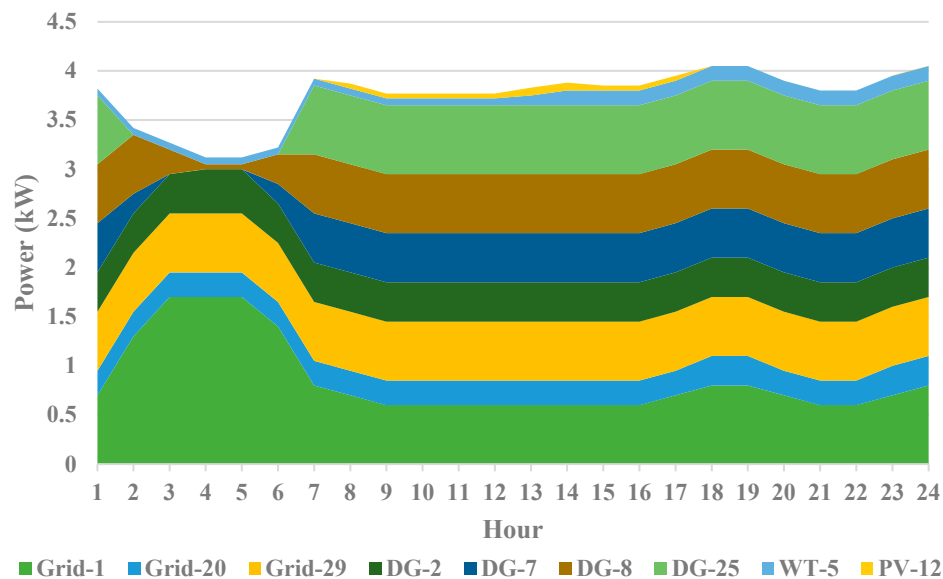


Figure 14. Unit involvement ratio in providing electrical loads for Case 3.

The involvement ratio of agents in Case 4 is shown in Figure 15. As a result of CHP generation, the MG has a higher chance of selling energy to the grid. MG profit in this case would be USD 5617.7. Figure 16 shows that CHP bus 8 produces the most heat because of its lower generation price. As shown in Figure 17, the IBOA algorithm solved the OPF problem by determining the system voltage curve, as well as the transition power of all system lines for maximal load demand in Case 4.

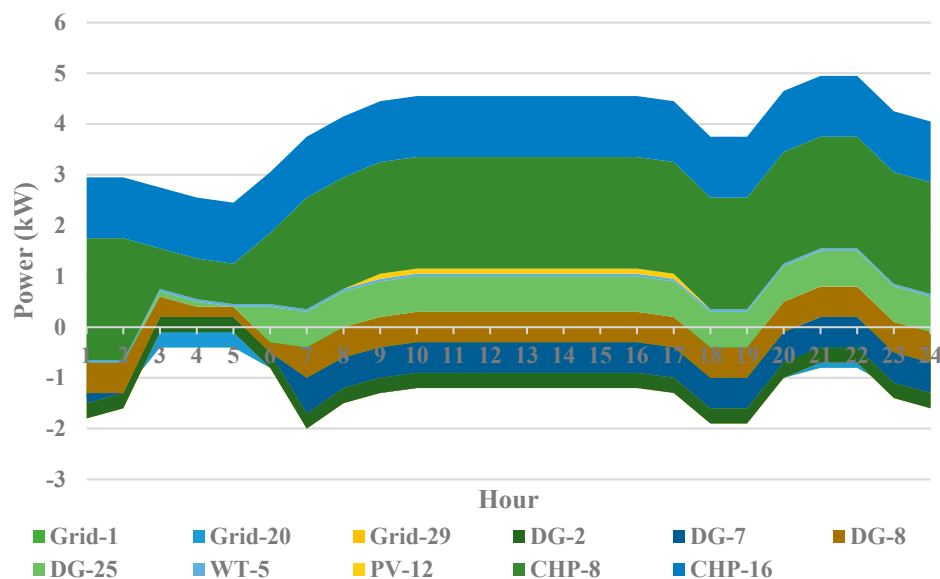


Figure 15. Unit involvement rate in providing electrical loads for Case 4.

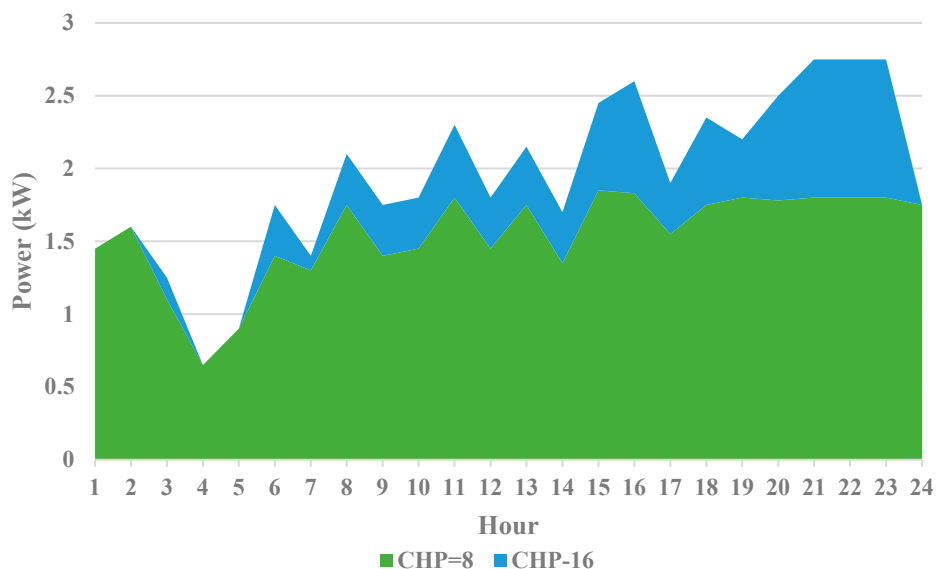
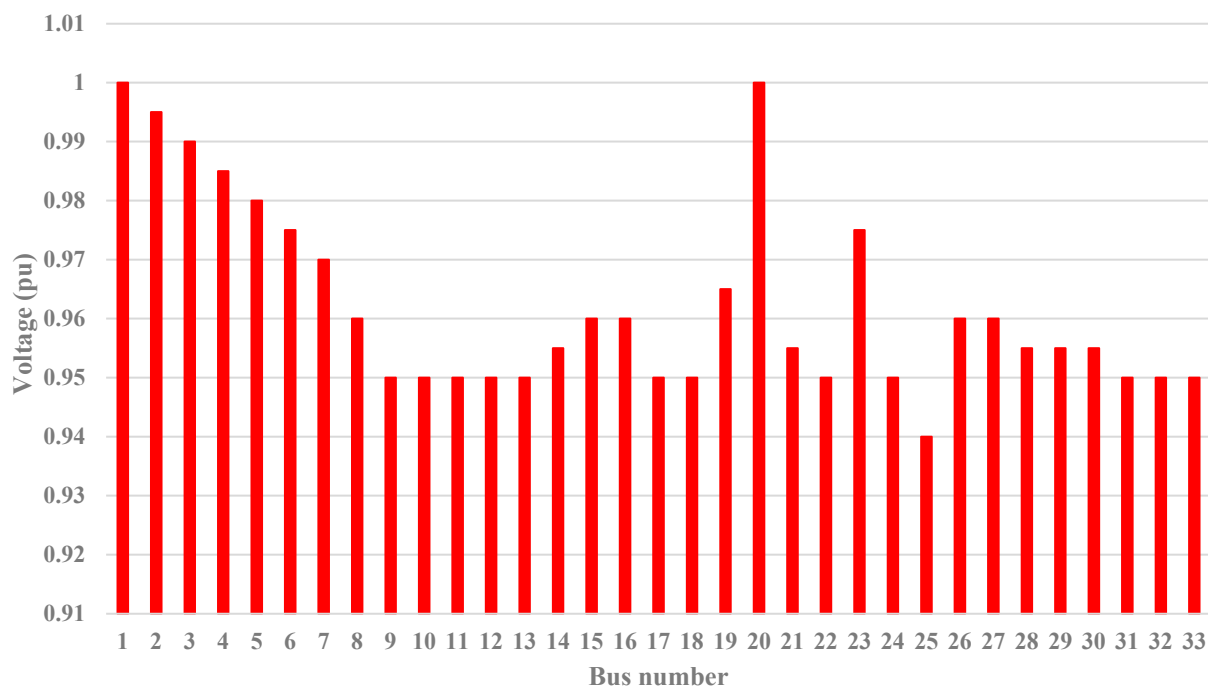


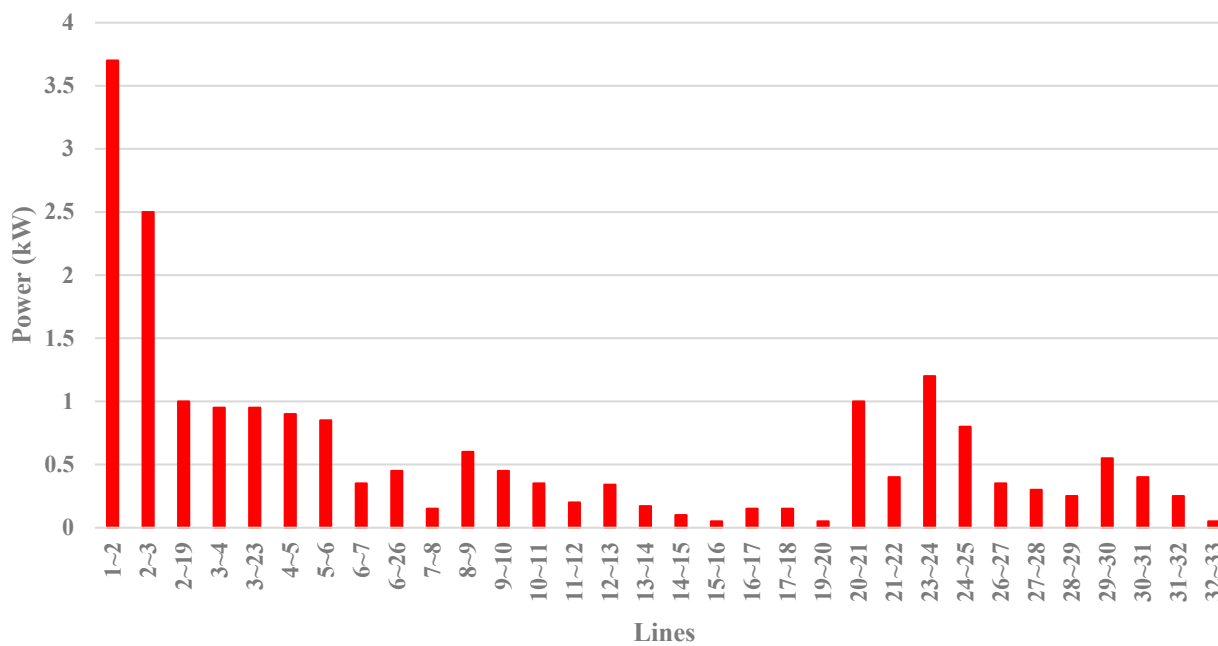
Figure 16. Involvement of CHP agents in buses 8 and 16 in providing heat load for Case 4.

The state of the suggested procedure in various cases is summarized in Table 10. This table illustrates MG income, price, and profit in four cases. Energy sales are the source of income, DC and OC are the costs, and profit is the difference. Clearly, Case 4 achieves the highest profit by implementing DSM and having different units in the MG. Table 11 compares the efficiency of the proposed approach with the other optimization schemes. According to the results, the suggested approach decreased prices by 57% and improved by 32% in comparison with the conventional BOA.

In order to reveal the convergence capability of the proposed model, Figure 18 shows the convergence curve of IBOA, BOA, and GA. According to this figure, the proposed algorithm first converges much sooner than the other algorithms.



(a)



(b)

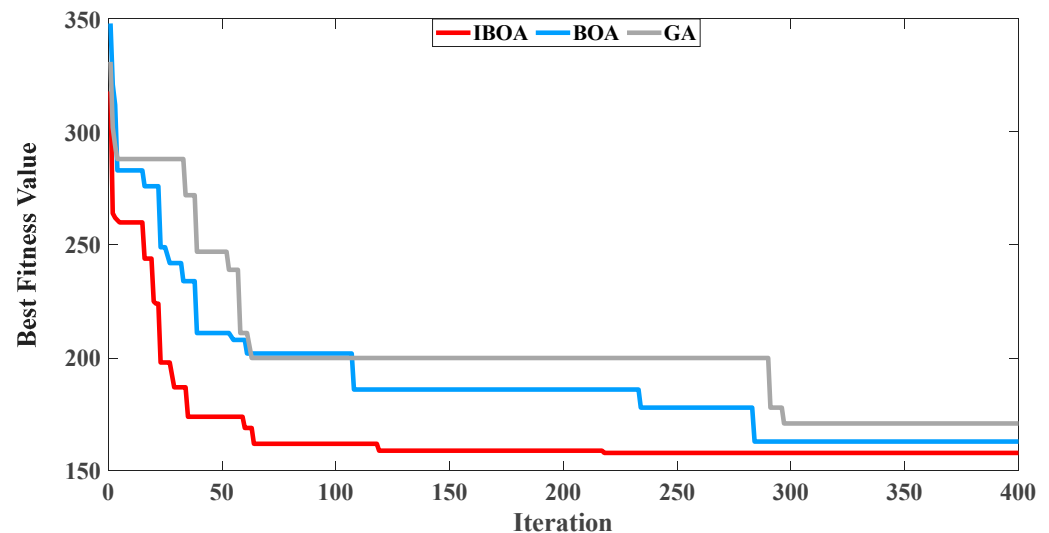
Figure 17. OPF outcomes using IBOA: (a) voltage curve, (b) line transition power variations for Case 4.

Table 10. The outcomes of profit and price of MGs in various cases.

Case No.		1	2	3	4
Coefficients	W_2	0	0	1	1
	W_1	1	1	1	1
Profit (\$)		2185.7133	5697.2560	2194.4243	5617.7067
Income (\$)		7492	7956.636	7185.814	7898.686
Price (\$)		5306.29	2349.38	4991.39	2280.98

Table 11. Comparing the outcomes of the suggested IBOA.

Algorithms	IBOA	BOA	GA
Price decrease (%)	57.01	50.7	25
Price (\$)	2281	2617	3978

**Figure 18.** The convergence curve of the proposed algorithm vs. others.

5. Conclusions

The present study models the optimum performance of MGs and DSM program deployment in the form of an optimization problem. As part of the optimization problem, the OF minimizes the price of MG operation and the DSM program implementation in order to improve user satisfaction. The optimization problem was solved by using an IBOA. There were three test networks that implemented the IBOA, resulting in the following outcomes. First, the DSM scheme reduced the operational costs of the whole MG. The second outcome is that the weight factor of the DSM increased, resulting in a decrease in the number and hours of load transfers and therefore raising the operational costs. Furthermore, the instantaneous cost of power can significantly affect MG's optimum performance. Lastly, this paper implemented the suggested approach on the IEEE 33-bus network in various case studies in order to demonstrate its effectiveness and compare the outcomes with classic BOA and GA algorithms. In conclusion, design characteristics include (1) providing shifting load rather than shedding and cutting load, and supplying critical load via MG; (2) improving the efficiency of IBOA compared with BOA; (3) assessing the price decrease effects of FC, MT, WT, PV, CHP, and BAT; (4) comparing IBOA to various algorithms; (5) reviewing the outcomes of the new approach under various conditions with the optimal efficiency decrease of 57%.

Author Contributions: Conceptualization, S.C.; Methodology, S.C.; Software, S.C.; Validation, S.C.; Formal analysis, S.C.; Investigation, B.D.; Resources, B.D.; Data curation, D.L.; Writing—original draft, D.L.; Writing—review & editing, D.L.; Visualization, D.L.; Supervision, D.L.; Project administration, D.L. All authors have read and agreed to the published version of the manuscript.

Funding: This research received no external funding.

Data Availability Statement: Data would be provided as per request.

Conflicts of Interest: The authors declare no conflict of interest.

References

1. Oliveira, V.; Tenfen, D.; Fernandes, R. Demand side management in Brazil: Brief history, lessons learned, status, challenges, and trends. *Renew. Sustain. Energy* **2023**, *183*, 113437.
2. Gelchu, M.A.; Ehnberg, J.; Shiferaw, D.; Ahlgren, E.O. Impact of demand-side management on the sizing of autonomous solar PV-based mini-grids. *Energy* **2023**, *278*, 127884.
3. Jokar, H.; Bahmani-Firouzi, B.; Simab, M. Bilevel model for security-constrained and reliability transmission and distribution substation energy management considering large-scale energy storage and demand side management. *Energy Rep.* **2022**, *8*, 2617–2629.
4. Damisa, U.; Nwulu, N.; Sun, Y. A robust energy and reserve dispatch model for prosumer microgrids incorporating demand response aggregators. *J. Renew. Sustain. Energy* **2018**, *10*, 055301.
5. Bustos, R.; Marín, L.G.; Navas-Fonseca, A.; Reyes-Chamorro, L.; Sáez, D. Hierarchical energy management system for multi-microgrid coordination with demand-side management. *Appl. Energy* **2023**, *342*, 121145.
6. Ali, L.; Muyeen, S.M.; Bizhani, H.; Ghosh, A. A multi-objective optimization for planning of networked microgrid using a game theory for peer-to-peer energy trading scheme. *IET Gener. Transm. Distrib.* **2021**, *15*, 3423–3434.
7. Topa, A.; Cruz, N.; Álvarez, J.; Torres, J. On the optimal demand-side management in microgrids through polygonal composition. *Sustain. Energy Grids Netw.* **2023**, *34*, 101066.
8. Karimi, H.; Niknam, T.; Dehghani, M.; Ghiasi, M.; Ghasemigarpachi, M.; Padmanaban, S.; Tabatabaee, S.; Aliev, H. Automated distribution networks reliability optimization in the presence of DG units considering probability customer interruption: A practical case study. *IEEE Access* **2021**, *9*, 98490–98505.
9. De Lara Filho, M.O.; Pinto, R.S.; De Campos, A.C.; Vila, C.U.; Tabarro, F.H. Day-Ahead Robust Operation Planning of Microgrids Under Uncertainties Considering DERs and Demand Response. In Proceedings of the 2021 IEEE PES Innovative Smart Grid Technologies Conference-Latin America (ISGT Latin America), Lima, Peru, 15–17 September 2021; IEEE: Piscataway, NJ, USA, 2021.
10. Abdunnasser, G.; Ali, A.; Shaaban, M.F.; Mohamed, E.E.M. Stochastic multi-objectives optimal scheduling of energy hubs with responsive demands in smart microgrids. *J. Energy Storage* **2022**, *55*, 105536.
11. Saffar, A.; Ghasemi, A. Energy management of a renewable-based isolated micro-grid by optimal utilization of dump loads and plug-in electric vehicles. *J. Energy Storage* **2021**, *39*, 102643.
12. Ebrahimi, S.R.; Rahimiyan, M.; Assili, M.; Hajizadeh, A. Home energy management under correlated uncertainties: A statistical analysis through Copula. *Appl. Energy* **2022**, *305*, 117753.
13. Ghasemi, M.; Kazemi, A.; Gilani, M.A.; Shafie-Khah, M. A stochastic planning model for improving resilience of distribution system considering master-slave distributed generators and network reconfiguration. *IEEE Access* **2021**, *9*, 78859–78872.
14. Eghbali, N.; Hakimi, S.M.; Hasankhani, A.; Derakhshan, G.; Abdi, B. Stochastic energy management for a renewable energy based microgrid considering battery, hydrogen storage, and demand response. *Sustain. Energy Grids Netw.* **2022**, *30*, 100652.
15. Castaño, J.C.; Garces, A.; Fosso, O.B. Short-Term Hydrothermal Scheduling With Solar and Wind Farms Using Second-Order Cone Optimization With Chance-Box Constraints. *IEEE Access* **2021**, *9*, 74095–74109.
16. Wang, Y.; Yu, H.; Yong, M.; Huang, Y.; Zhang, F.; Wang, X. Optimal scheduling of integrated energy systems with combined heat and power generation, photovoltaic and energy storage considering battery lifetime loss. *Energies* **2018**, *11*, 1676.
17. Chettri, P.K.; Sharma, K.; Dewan, S.; Acharya, B.K. Butterfly diversity in human-modified ecosystems of southern Sikkim, the eastern Himalaya, India. *J. Threat. Taxa* **2018**, *10*, 11551–11565.
18. Liu, B.; Zhou, B.; Yang, D.; Li, G.; Cao, J.; Bu, S.; Littler, T. Optimal planning of hybrid renewable energy system considering virtual energy storage of desalination plant based on mixed-integer NSGA-III. *Desalination* **2022**, *521*, 115382.
19. Liu, Z.; Hajiali, M.; Torabi, A.; Ahmadi, B. Novel forecasting model based on improved wavelet transform, informative feature selection, and hybrid support vector machine on wind power forecasting. *J. Ambient Intell. Humaniz. Comput.* **2018**, *9*, 1919–1931.
20. Alweshah, M.; Al Khalailah, S.; Gupta, B.B.; Almomani, A.; Hammouri, A.I. The monarch butterfly optimization algorithm for solving feature selection problems. *Neural Comput. Appl.* **2022**, *34*, 11267–11281.
21. Dashtdar, M.; Flah, A.; Hosseinimoghadam, S.M.S.; Kotb, H.; Jasińska, E.; Gono, R.; Leonowicz, Z.; Jasiński, M. Optimal Operation of Microgrids with Demand-Side Management Based on a Combination of Genetic Algorithm and Artificial Bee Colony. *Sustainability* **2022**, *14*, 6759.
22. Moghaddam, A.A.; Seifi, A.; Niknam, T.; Pahlavani, M.R. Multi-objective operation management of a renewable MG (micro-grid) with back-up micro-turbine/fuel cell/battery hybrid power source. *Energy* **2011**, *36*, 6490–6507.

Disclaimer/Publisher's Note: The statements, opinions and data contained in all publications are solely those of the individual author(s) and contributor(s) and not of MDPI and/or the editor(s). MDPI and/or the editor(s) disclaim responsibility for any injury to people or property resulting from any ideas, methods, instructions or products referred to in the content.